Advances in Nano Research, *Vol. 14, No. 4 (2023) 363-373*
https://doi.org/10.12989/anr.2023.14.4.363

Synergistic bond properties of new steel fibers with rounded-end from carbon nanotubes reinforced ultra-high performance concrete matrix

Nguyen Dinh Trung[1], Dinh Tran Ngoc Huy*[2], Dmitry Olegovich Bokov[3], Maria Jade Catalan Opulencia[4], Fahad Alsaikhan[5], Irfan Ahmad[6a] and Guljakhan Karlibaeva[7b]

[1]*National Economics University (NEU), Hanoi Vietnam*
[2]*Banking university HCMC Ho Chi Minh city Vietnam- International University of Japan, Niigata, Japan*
[3]*Institute of Pharmacy, Sechenov First Moscow State Medical University, 8 Trubetskaya St., bldg. 2, Moscow, 119991, Russian Federation; Laboratory of Food Chemistry, Federal Research Center of Nutrition, Biotechnology and Food Safety, 2/14 Ustyinsky pr., Moscow, 109240, Russian Federation*
[4]*College of Business Administration, Ajman University, Ajman, United Arab Emirates*
[5]*Department of Clinical Pharmacy, College of Pharmacy, Prince Sattam Bin Abdulaziz University, Alkharj, Kingdom of Saudi Arabia*
[6]*Department of Clinical Laboratory Sciences, College of Applied Medical Sciences, King Khalid University, Abha, Saudi Arabia*
[7]*Department of Physics Teaching Methods, Tashkent State Pedagogical University named after Nizami, Bunyodkor street 27, Tashkent, Uzbekistan*

(*Received November 2, 2021, Revised November 8, 2022, Accepted November 17, 2022*)

Abstract. A novel type of steel fiber with a rounded-end shape is presented to improve the bonding behavior of fibers with Carbon Nanotubes (CNT)-reinforced Ultra-High Performance Concrete (UHPC) matrix. For this purpose, by performing a parametric study and using the nonlinear finite element method, the impact of geometric characteristics of the fiber end on its bonding behavior with UHPC has been studied. The cohesive zone model investigates the interface between the fibers and the cement matrix. The mechanical properties of the cohesive zone model are determined by calibrating the finite element results and the experimental fiber pull-out test. Also, the results are evaluated with the straight steel fibers outcomes. Using the novel presented fibers, the bond strength has significantly improved compared to the straight steel fibers. The new proposed fibers increase bond strength by 1.1 times for the same diameter of fibers. By creating fillet at the contact area between the rounded end and the fiber, bond strength is significantly improved, the maximum fiber capacity is reachable, and the pull-out occurs in the form of fracture and tearing of the fibers, which is the most desirable bonding mode for fibers. This also improves the energy absorbed by the fibers and is 4.4 times more than the corresponding straight fibers.
Keywords: bond strength; CNT-reinforced; novel steel fibers; pull-out behavior; UHPC

1. Introduction

Modern investigators in concrete technology are devoted to developing new materials with enhanced mechanical properties and improved durability (Jarach *et al*. 2021, Aghajanian *et al*. 2021, Esmaeili and Andalibi 2021). Since the discovery of nanoparticles, interest in nano-particles has increased rapidly because of their individual and superior mechanical properties (Aghakhani and Naderian 2015, Dhiman *et al*. 2022, Shekhovtsova and Korolev 2022, Sher *et al*. 2022). Nanomaterials, such as CNT, Al_2O_3, Fe_2O_3, and TiO_2 nanoparticles have been employed to enhance the mechanical properties of engineering materials due to their high elastic modulus and tensile strength of materials (Rezaee and Maleki 2015, Dmytro *et al*. 2020, Maleki *et al*. 2022). Furthermore, adding fibers to cement-based matrices improves flexibility and cracking resistance, as well as increasing energy absorption and toughness of these composites compared to fiber-free cement-based matrices. When cracks propagate in cementitious matrices, the fibers prevent the rapid growth of one or more cracks and their interconnection by using the crack bridging mechanism. However, due to the random distribution of fibers in the matrix, the fibers are not always perpendicular to the resulting cracks and are positioned in different directions. When a crack opens in the matrix, the fibers are loaded at different angles and embedded lengths, causing other mechanisms to occur when these inclined fibers are pulled out of the matrix. Due to the significant effect of the pull-out behavior of individual fibers from the matrix on the overall behavior of the composites, having accurate knowledge of this phenomenon and its details is very important. Many researchers have considered this issue in recent years.

Steel fibers are often added to concrete to improve the overall material performance (Baniya *et al*. 2021, Naderi and Zhang 2022, Sharma *et al*. 2022). The main important effect of fibers as reinforcement is to influence and control the tensile cracking of concrete (Parashar and Gupta 2021). Similar to steel rebars, the bonding between fibers and cement matrix can be divided into chemical adhesion, physical friction, and mechanical anchorage (Ming *et al*.

*Corresponding author, MBA,
E-mail: Dtnhuy2010@gmail.com;
atenaatashsokhan@yahoo.com
[a] Assistant Professor, E-mail: irfancsmmu@gmail.com
[b] Professor, Ph.D.

ISSN: 2287-237X (Print), 2287-2388 (Online)

2021, Dinet *et al*. 2021, Qi *et al*. 2018, Abdallah *et al*. 2018, Dahi Taleghani *et al*. 2013). Mechanical anchorage is caused by the deformation of steel fibers and matrices and plays a crucial role in the pull-out load of the fibers. Increasing the pull-out strength of the fibers enhances the tensile strength of concrete, which is usually about 8MPa. Conventional steel microfibers used in reinforcing cement-based composites have a tensile strength of about 2000MPa (Graybeal 2008), and for straight steel microfibers with a diameter of 0.2mm and length of 13mm, only 981MPa of tensile stress is applied by the concrete matrix (Yang *et al*. 2019, Müssig and Graupner 2021). This means that the fibers total tensile capacity is not used. In other words, the straight steel fibers used in concrete are usually exposed to pull-out, and stress is applied to them with less than half the tensile strength. Therefore, new geometries of steel fibers are needed to take advantage of their maximum tensile capacity. Accordingly, several studies (Qi *et al*. 2018, Poveda *et al*. 2020, Ebrahimi and Habibi, 2017, Du *et al*. 2021, Timesli, 2021) have presented different geometries for fibers, and improved bond strength with different types of concrete.

Tai *et al*. (2016) studied the pull-out behavior of straight, hooked, and twisted steel fibers using experimental static loading tests. They also investigated inclination angles in the range of 0 to 60°. Their research findings show that the deformed fibers perform better than straight fibers. Wille *et al*. (2012) showed that the application of twisted steel fibers significantly improves the flexural and tensile behavior of fiber concrete. Ebrahimi and Habibi (2017) studied the pull-out behavior of superelastic fibers with different end-shapes from cement mortar. Their study experimentally examined four different end-shapes, including straight, crimped-end, N, and L-shaped, with spearhead fibers. Their research indicated that crimped-end fibers have better pull-out strength than other specimens. Schmidt and Fehling (2005) investigated the bond-slip response of new half-hooked steel fibers. They studied the effect of fiber hook angle and showed that the end-angle of the fibers has a significant impact on the pull-out performance of the fibers and suggested the suitable angle to be 45°. Riahi *et al*. (2021) investigated the effect of alumina coating on fibers cohesion of steel fibers. Esmaeili *et al*. (2021) studied the impact of the end-shape of hook-shaped steel fibers on the pull-out strength of fibers in polymer concrete, experimentally and numerically. They defined the cohesion properties between the fibers and the matrix in numerical modeling using the Interfacial transition zone. The findings of their study confirmed that by increasing the fibers angle in the range of 0 to 90°, the pull-out load of the fibers increases by about 35%. Using the analytical model, Zerrouki *et al*. (2020) provided an explicit relation for the pull-out load of new 3D/ 4D/ 5D steel fibers under tensile loading. In the most recent studies, Kim *et al*. (2021) studied the performance of the new curved steel fibers using pull-out tests of ultra-high-performance concrete. Their results showed that the new fibers have excellent performance compared to conventional fibers, and matrix spalling was observed in the fiber pull-out test. Ding *et al*. (2021) experimentally studied the effect of five common types of steel fiber geometric shapes on bond strength. Their study showed that the maximum stress reated in crimped steel fibers with a circular cross-section is 1150MPa. Lee *et al*. (2016) and Won *et al*. (2015) fabricated arch-type steel fibers and showed that the pull-out strength of these fibers is better than hook-shaped steel fibers. The literature review shows that in most of the proposed fiber geometries, although the pull-out strength is significantly improved compared to straight fibers, the fibers are pulled out of the cement matrix. This pull-out type prevents the fibers from yielding to the yield strength and thus does not use their maximum tensile strength capacity.

Table 1 Mixture proportion of CNT-reinforced UHPC matrix

Mixed design components	(kg/m$^{3)}$
Portland Cement Type II	665
Micro Silica	210
Quartz powder	290
Silica Sand	1030
Super Plasticizer (3%)	20.2
Water (Liter)	180
CNT	2.03

Table 2 Dimensions and mechanical properties of the CNT

Type	SWCNT
Specific gravity (g/cm^3)	2.45
Surface area (m^2/g)	230
Inner diameter (nm)	8.5
Carbon content (%)	>96.0
Length (μm)	40
Elastic modulus (GPa)	1280
Tensile strength (GPa)	160

This study evaluated the pull-out performance of CNT-reinforced UHPC samples with the newly developed rounded-end shape steel fibers to verify their feasibility and effectiveness. Accordingly, the novelty of this numerical study is proposed a novel shape for steel fiber and investigate the effects of its geometry on the bond properties of new steel fiber with carbon nanotubes reinforced ultra-high performance concrete matrix. By performing numerical simulations, the effect of fibers geometric parameters and their end-shape geometry on the pull-out behavior of the fibers has been studied. Also, the outcomes of experimental pull-out analysis have been used to validate the results of the finite element model. For this purpose, the steel fibers with rounded-ends are fabricated, and then the pull-out test is conducted on the standard specimen.

2. Experimental tests

2.1 Mixing plan

A CNT-reinforced UHPC matrix with compressive

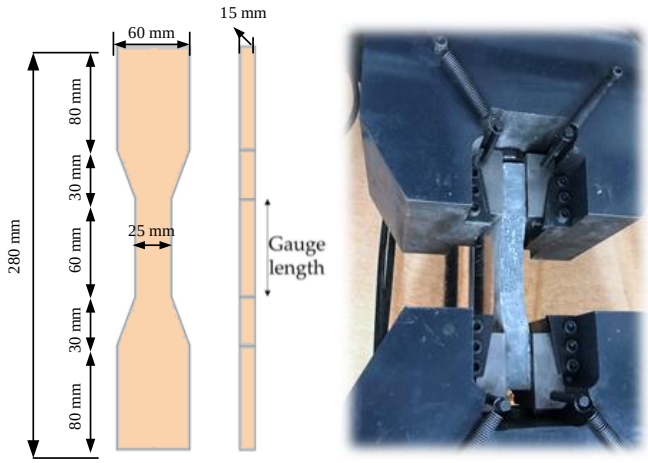

Fig. 1 Geometric characteristics of the tensile test specimen and direct tensile test machine

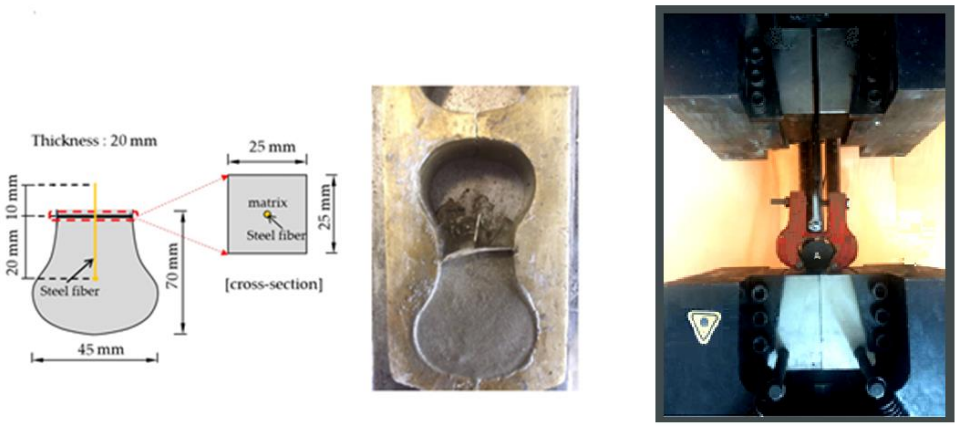

Fig. 2 The pull-out specimen, geometry, and the pull-out experimental setup

strength of 146 MPa was used for the experimental pull-out test. Table 1 shows the mass ratios of the matrix used. Type II cement is used in the construction of the UHPC. Also, silica aggregates with dimensions of 0.01 to 0.5mm have been used as fine aggregates.

Carbon nanotubes have a very high tensile strength compared to concrete. Single-walled carbon nanotubes have been used in the present study. CNT were purchased from the company "Nanografi Nano Teknoloji AS,, Turkey." The dimensions and mechanical properties of the CNT are listed in Table 2.

2.2 Compressive strength test

Three cubic specimens (dimensions 50×50×50mm) were tested experimentally. An experimental compressive strength test was conducted using a universal machine with a loading rate of 0.1mm/min to evaluate the compressive strength and stress-strain curve of the cementitious composite.

2.3 Tensile strength test

Tensile properties of the CNT-reinforced UHPC used were determined using the direct tensile test of dog-bone specimens. Fig. 1 demonstrates the geometric characteristics of the tensile test specimen and how it is placed in the universal machine. To determine the tensile stress-strain curve results average of the three different specimens was used.

2.4 Pull-out test

In the present research, an experimental pull-out analysis of the novel rounded-end (RE) steel fibers was performed to validate the model. The pull-out specimens have a height, width, and cross-sectional area of 70mm, 45mm, and 25×25 mm, respectively. The specimens, their geometry, and the pull-out experimental setup are shown in Fig. 2. The universal test machine with a maximum load of 10 kN and a 0.05 mm/min loading ratio has been used to apply the pull-out load. One end of the dog-bone specimen is placed inside the fixture, and the tensile load is applied to the fibers using the other jaw of the machine. A dynamometer with an accuracy of 0.5N was used to measure pull-out load. The steel fibers, the ends of which have been rounded using a mechanical press, are placed in the middle of the specimen cross-section. The embedded length of the fibers inside the concrete is 20mm. The geometric shape of the RE fibers presented in the present

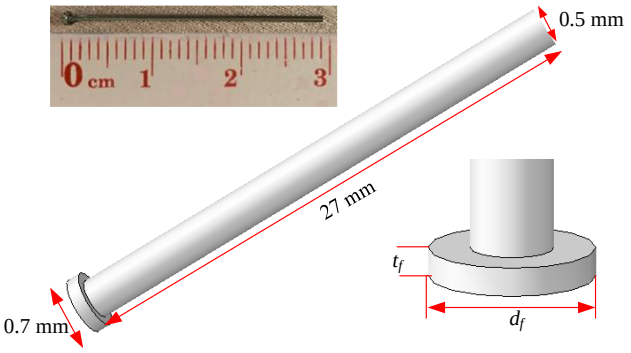

Fig. 3 The novel RE steel fibers

Table 3 Geometric and physical properties of the RE steel fibers

Parameter	Value
fiber diameter	0.5mm
fiber length	30mm
d_f	0.7mm
t_f	0.4
Aspect ratio	100
f_{ft}	1280MPa
E_f	206GPa

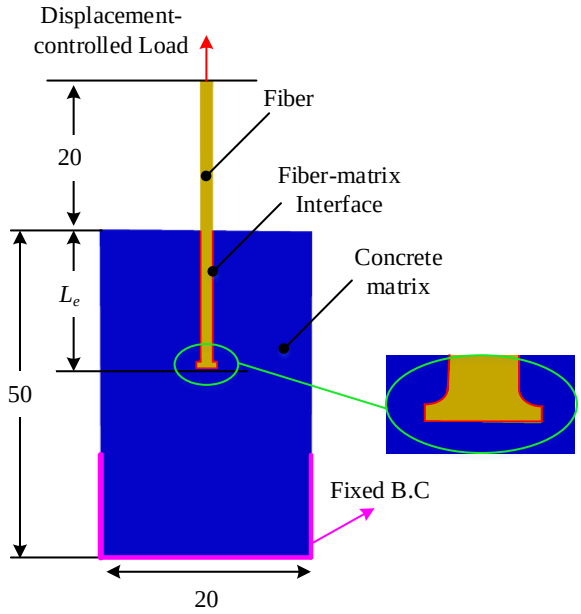

Fig. 4 Geometric characteristics of the finite element pull-out model (dimensions in mm)

research is shown in Fig. 3. This type of fiber is fabricated using straight steel fibers with a length of 30mm and a diameter of 0.3mm. Its geometric and physical characteristics such as density, elastic modulus, shear modulus, and failure strains are given in Table 3. It should be noted that in the current study, the pull-out test was performed for both types of straight and rounded-end steel fibers.

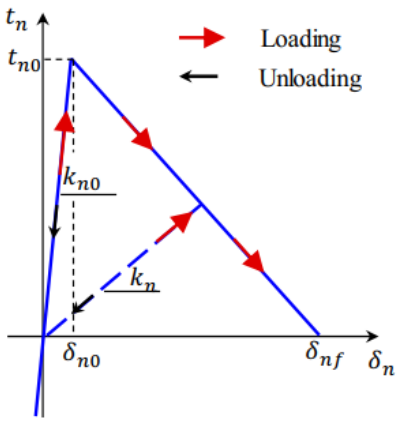

Fig. 5 Traction-separation law (Dahi Taleghani *et al.* 2013)

3. Finite element modeling

In the current research, the finite element method was utilized to study the pull-out performance of the new RE steel fibers from cement composite. The main focus of the present study is on the relationship between load displacement and energy absorbed during the pull-out process. Fig. 4 demonstrates a geometric model of pulling the fibers out of concrete in which the steel fibers are embedded in a cylindrical matrix. According to Fig. 4, the sections in pull-out modeling are concrete matrix, steel fiber, and fiber-concrete interface. Simillarly to the experimental test, the pull-out load is applied at a rate of 0.05mm/min to the outer ends of the fibers. Additionally, the lower part of the concrete matrix is considered completely constrained.

3.1 Interaction of fibers and matrix

Here, the surface-to-surface contact model and the cohesive zone model (CZM) criterion are used to simulate the interplay between the concrete and fibers. This contact model can consider all the mechanisms of bonding (adhesion, debonding, and friction) during the pull-out of the fibers. Accordingly, the linear biaxial uncoupled elastic traction–separation interaction model is used. In this method, the traction stress tensor (t) and the related slip (δ) are related in terms of the elastic stiffness matrix (K) according to Equation (1). Stiffness is defined in two directions of vertical n and shear s axes, which is shown in Fig. 5 as a schematic of this behavioral model.

$$t = \begin{Bmatrix} t_n \\ t_s \end{Bmatrix} = \begin{bmatrix} k_{nn} & 0 \\ 0 & k_{ss} \end{bmatrix} \begin{Bmatrix} \delta_n \\ \delta_s \end{Bmatrix} = K\delta \quad (1)$$

The three parts of the traction-separation curve are divided into linear elasticity, linear softening, and debonding. Fig. 5 demonstrates critical separation and failure separation distances (δ_c and t_c), and dilation angle δ_f. Also, the section below the traction-separation diagram shows the separation failure energy. According to Fig. 5, the following relation can be presented for interfacial behavior:

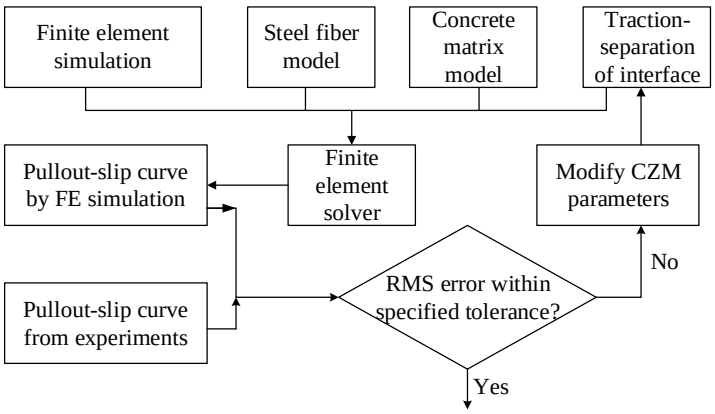

Fig. 6 Inverse finite element method based on optimization problems to estimate the CZM parameters between fibers and cement matrix

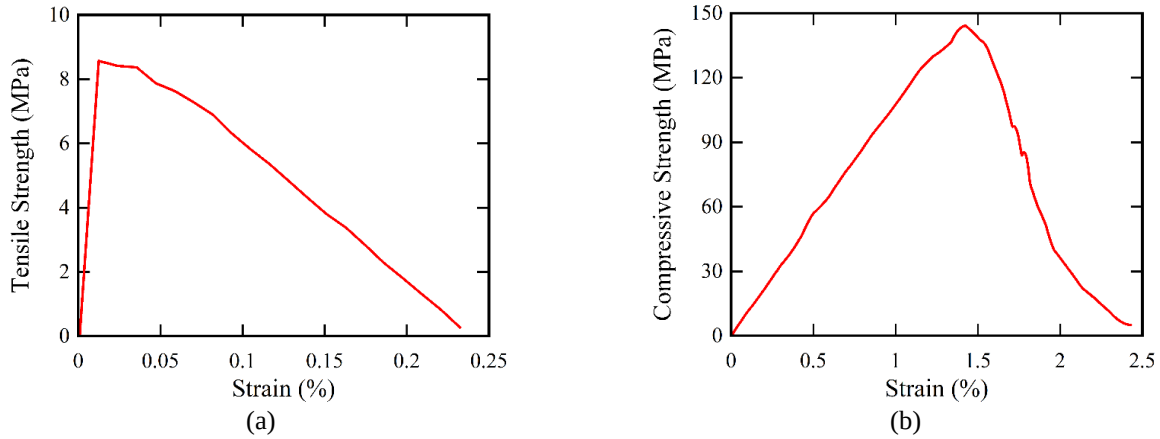

Fig. 7 (a) Experimental tensile stress-strain curve and (b) compressive stress-strain curves of CNT-reinforced UHPC

Table 4 Mechanical properties used for CNT-reinforced UHPC

Concrete properties	Compressive strength	Modulus of elasticity	Tensile strength	Fracture energy
	146.3 MPa	55.45 GPa	8.32 MPa	0.1 N/mm
CDP parameters	ψ	e	$\frac{f_{bo}}{f_{co}}$	K_c
	36	0.1	1.16	0.67

$$\tau = \begin{cases} \tau_{n0}\left(\dfrac{\delta}{\delta_{n0}}\right) & 0 \le \delta \le \delta_{n0}\text{(linear elasticity)} \\ \tau_{n0}\dfrac{(\delta-\delta_{nf})}{(\delta_{n0}-\delta_{nf})} & \delta_{n0} \le \delta \le \delta_{nf}\text{(linear softening)} \\ 0 & \delta_{nf} < \delta\text{(debonding)} \end{cases} \quad (2)$$

With three parameters δ_c, t_c and δ_f, the bonding behavior of the fibers to the cement matrix can be defined.

3.2 Estimation of the CZM utilizing inverse finite element method

The CZM parameters consist of three parameters δ_c, t_c, and δ_f evaluated employing the method mentioned in Fig. 6. Since the CZM considers the three characteristics of chemical adhesion, debonding, and friction in the simulations, the straight fiber pull-out test results are used to predict these parameters for new fibers. Similar to the experimental test, the fibers embedded length L_e = 20 mm is considered. The parameters of the CZM are estimated based on the inverse finite element method, which was first proposed by Rajeshkumar *et al.* (2021) to predict some mechanical characteristics such as elastic modulus and viscosity. Fig. 6 shows the steps for estimating the CZM parameters. In this method, which is based on optimization methods, the factors are obtained by minimizing the RMS error in the experimental and numerical outcomes.

3.3 Mechanical properties of materials

In the current research, the behavioral model of concrete damage plasticity (CDP) has been used to simulate the nonlinear behavior of concrete materials. The factors in this behavioral model include plastic potential eccentricity, dilation angle ψ, the ratio of biaxial compressive strength to the uniaxial compressive strength of concrete $\frac{f_{bo}}{f_{co}}$, loading coefficient K_c, and viscosity. Table 4 shows the mechanical properties used for concrete. In addition, the tensile and compressive behavior of concrete obtained from the

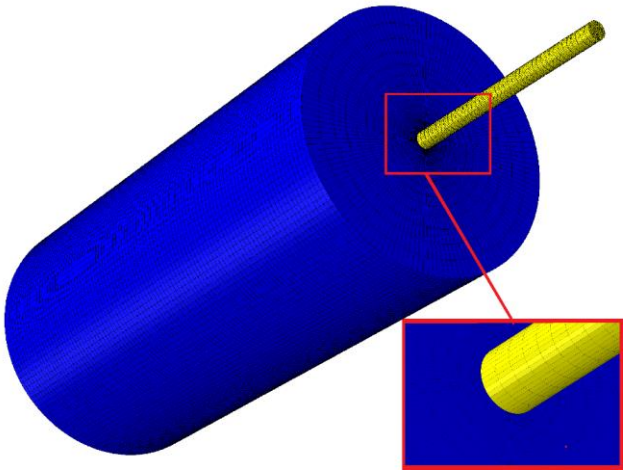

Fig. 8 Meshed model of the fibers pull-out with fine elements around the fibers

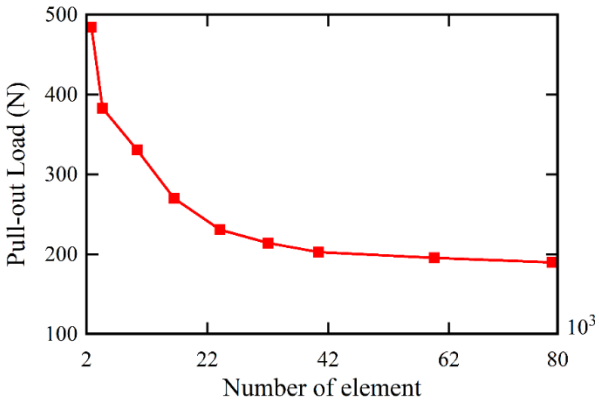

Fig. 9 Grid independency

Table 4 Mechanical properties used for CNT-reinforced UHPC

	t_c	δ_c	δ_f
Steel fiber	34.15 MPa	2.3×10^{-3}mm	0.34 mm

experimental tests is introduced to ABAQUS commercial code using the stress-strain curves shown in Fig. 7. For the steel fibers, the perfect elastic-plastic model was used. Density, Young's modulus, and Poisson's ratio of the fibers are 7800kg/m^3, 207GPa, and 0.3, respectively. Also, the yield stress of the used fibers is 2580MPa.

3.4 Mesh sensitivity

Determining the appropriate size of the grid elements is very important to achieve accurate results with the lowest computational cost. According to Fig. 8, C3D20R elements have been used for meshing in the present research. A grid independence investigation was performed to determine the appropriate size of the elements, and a summary of the results is provided in Fig. 9. The pull-out load is plotted in terms of the element number. According to the results, it is observed that with increasing the number of elements, the pull-out load converges to a specific value, and element numbers greater than 42000 have little effect on the results. Therefore, in this study, the mentioned element number is used.

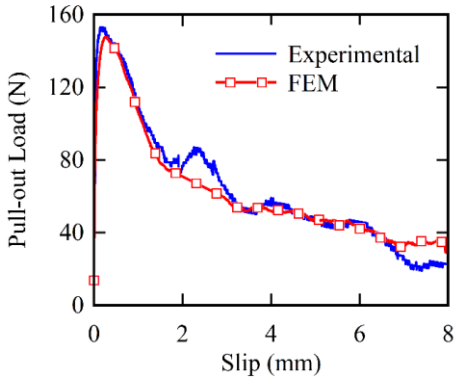

Fig. 10 Experimental and the numerical result of pull-out load with slip for the straight steel fibers

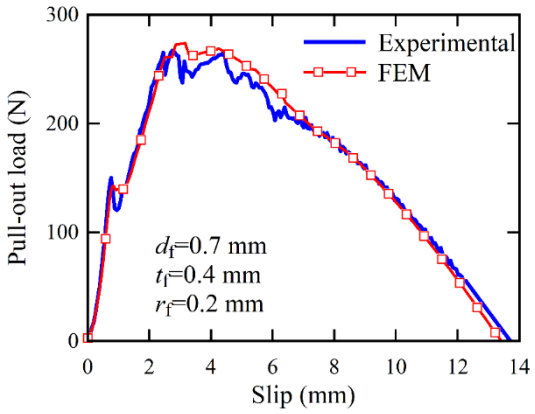

Fig. 11 Experimental and the numerical result of pull-out load variations with slip for RE steel fibers

4. Results and discussion

4.1 CZM parameters

The CZM parameters consist of three parameters δ_c, t_c and δ_f are evaluated employing the method mentioned in Fig. 6. In the iteration process, based on the reference results (Riahi *et al*. 2021, Kaloop *et al*. 2022), the initial values for the three parameters δ_c, t_c and δ_f are considered to be 2.8×10^{-3}mm, 8.23MPa, and 12.8×10^{-3}mm, respectively. The RMS error of the finite element method (FEM) and experimental pull-out load is calculated for all iterations. The iteration process stops when the RMS error reaches less than 3%. In the present study, after 23 iterations, the optimization process estimates the CZM parameters as presented in Table 4. Fig. 10 demonstrates pull-out load variations with slip obtained from the simulations and experimental results performed on the straight steel fibers. As can be seen, the FEM results are reasonably consistent with the experimental ones, and the pull-out load difference results are less than 2%.

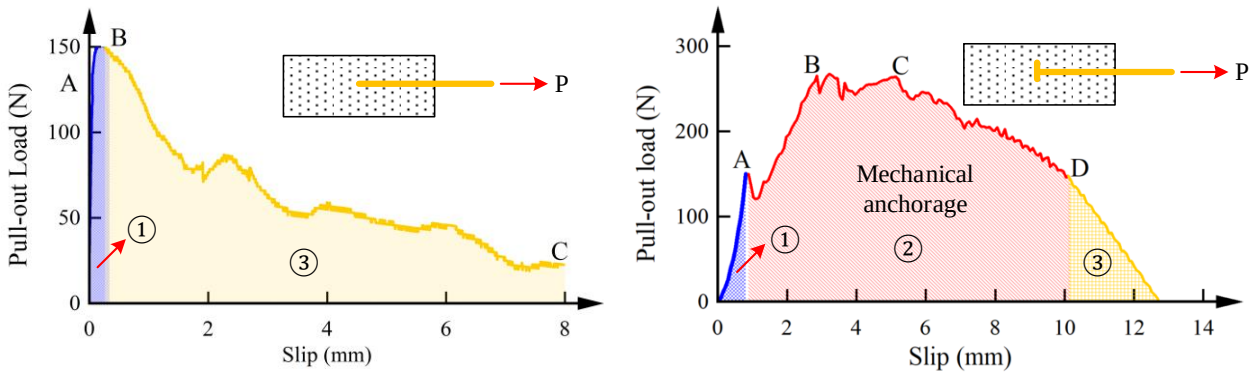

Fig. 12 Pull-out response for the straight and RE steel fibers ($d_f = 0.7$mm, $t_f = 0.4$mm and $r_f = 0.2$mm)

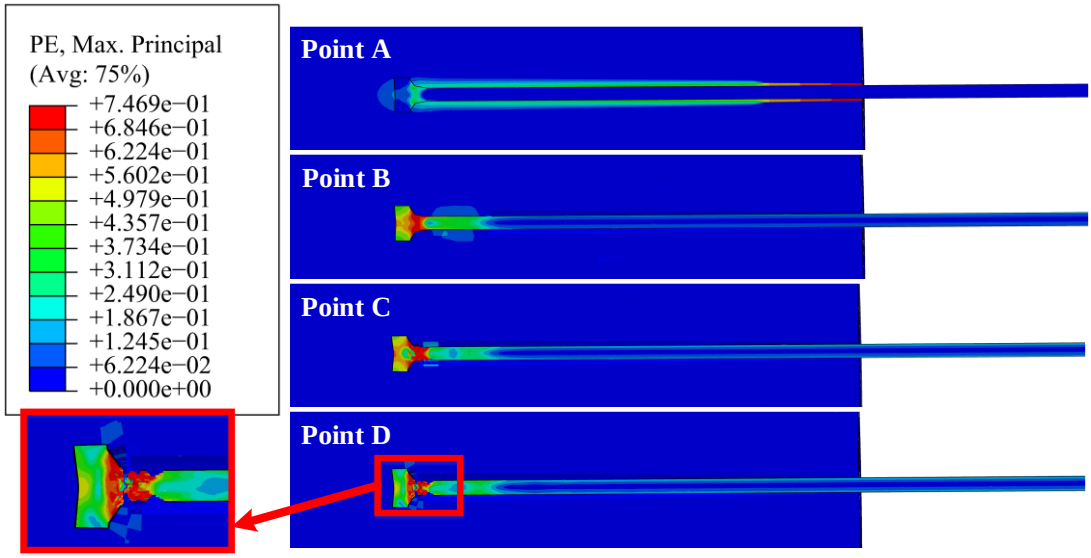

Fig. 13 Plastic strain distribution in positions A, B, C, and D (Fig. 11) for the RE fibers

4.2 Validation

In Fig. 11, the RE fibers pull-out results of the FEM are compared with the results of the experimental tests for $l_e = 20$mm, $d_f = 0.7$mm, $t_f = 0.4$mmand $r_f = 0.2$mm. It can be seen that in the linear elastic zone, the FEM and experimental results are entirely consistent, while after debonding, the results become somewhat different. The reason for this slight error between the FEM and experimental results is due to not taking into account the uncertainties in simulating the mechanical behavior of cementitious composites and fibers. Pull-out load and failure energy estimated errors are 3.8% and 2.9%, respectively, which are acceptable.

4.3 Behavior of the straight and RE steel fibers

The presence of the steel fibers rounded ends causes the pull-out performance of the RE fibers to be quite different from straight fibers. Fig. 12 shows the pull-out response of the straight and RE steel fibers with $d_f = 0.7$mm, $t_f = 0.4$mmand $r_f = 0.2$mm. For the straight fibers, pull-out strength consists of the two adhesive strength (Zone 1, Fig. 12a) and frictional bond (Zone 3, Fig. 12b) zones. As can be seen from Fig. 12a, in this type of fiber, after reaching the maximum load (point B), a rapid drop occurs in the curve, and the bond strength disappears. For the RE fibers, the behavior is completely different. In zone 1 there is adhesive strength, which in point A disappears completely. After the adhesive strength disappears at point A, debonding begins at the outer ends of the fibers. Next, the mechanical anchorage is the main factor in the pull-out process (Zone 2 in Fig. 11). In this zone (from point A to points B and C), embedding the rounded ends inside the concrete causes pull-out strength, and an acceptable tensile strain is created in the fibers. As can be seen, this zone exists only in this type of fibers. After the maximum load (point B), plastic strain is created in the steel fibers, and with increasing the load, the steel fibers start to debond. In path CD, the damage of the fibers increases, and finally, at point D, the fibers are completely debonded. After fiber debonding, continued pull-out is associated with frictional strength. This fiber deformation behavior is demonstrated in Fig. 13, which shows the plastic strain distribution at positions A, B, C, and D for the RE fibers. As can be seen, due to the strong mechanical anchorage, the fibers are prematurely ruptured at their ends. In addition, a quantitative examination of the pull-out diagrams of the straight and RE fibers shows that

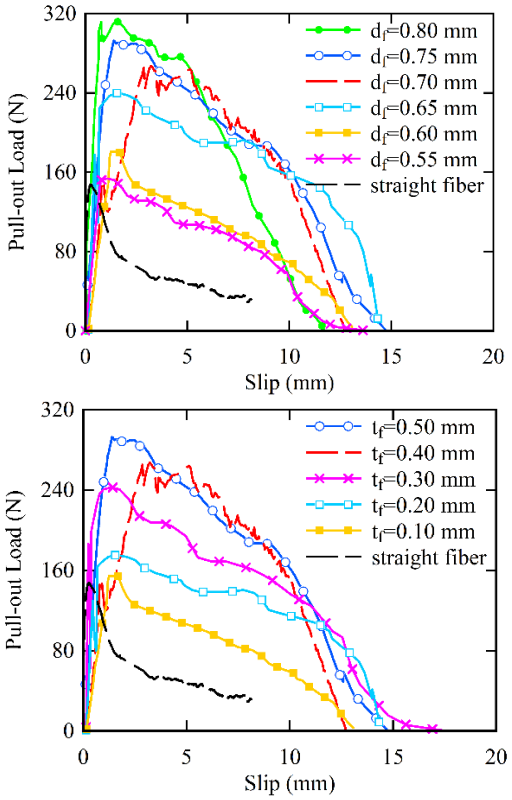

Fig. 14 Effect of geometric characteristics of the RE fibers: (a) d_f and (b) t_f on the load-slip curve

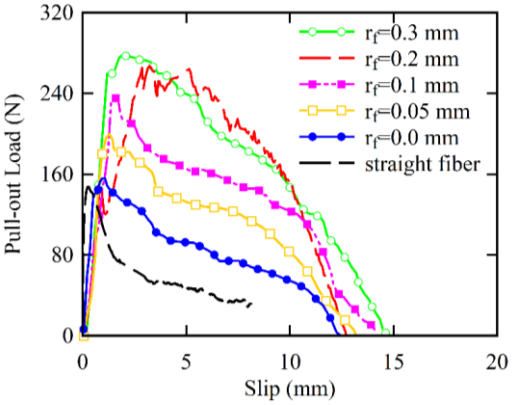

Fig. 15 Effect of fillet radius of the RE fiber on pull-out load

the RE fibers have a much higher pull-out load and absorbed energy compared to the straight fibers. According to Fig. 12, it can be seen that for the same conditions, the pull-out load and the absorbed energy of the RE fibers are 78% and 345% higher compared to the straight steel fibers, respectively. Meanwhile, the impact of factors affecting the pull-out performance of the RE fibers is discussed as follows.

4.4 Geometry analysis

Figs. 14 and 15 show the effect of the fiber ends geometric characteristics, including three parameters d_f, for $L_e = 20$mm and fibers diameter 0.5mm. By investigating

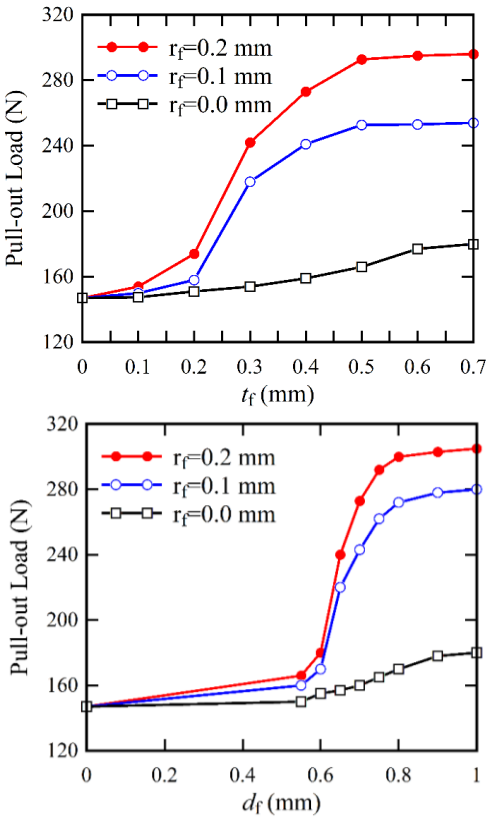

Fig. 16 Pull-out load variations with geometric characteristics: (a) effect of d_f, (b) effect of t_f

the pull-out performance of the straight and RE fibers, it is concluded that for the straight fibers, sliding occurs outwards, and as a result, the failure is of slipping type. In the RE fibers, besides chemical adhesion and frictional stability, mechanical anchorage in the polymer composite and the fiber end parts cause the bond strength increment. As can be seen, among the bonding mechanisms, the mechanical bonding of the RE fibers with cementitious composites is of significant parameter since it causes the greatest bond stress. In the coupling procedure, load transfer is performed by engaging the rounded ends of the fibers and the mechanical anchorage in the fibers and the cementitious composite. This causes the fibers to rupture in the proper geometric properties at the ends of the fibers. Because the rupture in the fibers is caused by enduring stresses higher than the ultimate tensile stress, the maximum tensile capacity of the fibers is used. Also, according to the results, it is observed that with increasing d_f, the maximum pull-out load also increases due to the increased mechanical anchorage of the fibers with cementitious composites. It should be noted that with increasing d_f, its effect on increasing the pull-out load decreases. Similar results are seen for the effect of t_f and r_f parameters. For small values of the parameters d_f, t_f and r_f, the fibers pull-out is slipping, and by increasing them to a specific value, the pull-out slip of the fibers occurs after the fibers are ruptured. Therefore, the effect of high values of these parameters on the pull-out load will be logical, the results of which are demonstrated in Fig. 16. The results show that the

Table 5 Pull-out response key parameters

No	d_f	t_f	r_f	Pull-out Load (N)	Critical Separation (mm)	Pull-out Work (N/mm)	Bond Stress (MPa)	fiber-stress (MPa)	strength use efficiency
1	0.7	0.4	0	155.6	0.93	1.03	4.96	792.87	0.62
2			0.05	200.0	1.28	1.42	6.37	1019.11	0.80
3			0.10	236.2	1.70	1.78	7.52	1203.57	0.94
4			0.15	245.1	2.06	1.94	7.82	1248.92	0.98
5			0.20	273.3	3.17	2.43	8.70	1392.61	1.09
6			0.30	278.9	1.95	2.34	8.88	1421.15	1.11
7	0.7	0.0	0.2	147.6	0.27	0.49	4.70	752.10	0.59
8		0.1		154.2	1.24	1.03	4.91	785.73	0.61
9		0.2		175.4	1.60	1.76	5.59	893.76	0.70
10		0.3		242.3	1.37	2.25	7.72	1234.65	0.96
11		0.4		273.3	3.17	2.43	8.70	1392.61	1.09
12		0.5		292.7	1.39	2.65	9.32	1491.46	1.17
13	0.55	0.4	0.2	153.6	1.08	1.04	4.89	782.68	0.61
14	0.60			180.5	1.24	1.25	5.75	919.75	0.72
15	0.65			240.1	1.60	2.17	7.65	1223.44	0.96
16	0.70			273.3	3.17	2.25	8.70	1392.61	1.09
17	0.75			292.7	1.39	2.57	9.32	1491.46	1.17
18	0.80			301.2	1.46	2.12	9.59	1534.78	1.20
19	Straight fiber	-	-	147.6	0.27	0.49	4.70	752.10	0.59

pull-out load converges to a specific value in the RE fibers for d_f and t_f values greater than 0.8 and 0.5, respectively. In addition, it is observed that the radius of the fillet at the rounded ends significantly improves the fibers pull-out behavior. For r_f=0, the effect of the fibers rounded ends on pull-out load is not very noticeable. Although the rounded ends significantly strengthen the mechanical bonding of the fibers with the cementitious composite, in this case, due to the concentration of stress, the fibers will rupture by small amounts of pull-out load. Therefore, this type of fibers will have excellent performance in the presence of fillets at the joint. For example, for r_f=0 and r_f=0.2, by increasing d_f from 0.5mm to 1mm, the pull-out load increases by 16% and 70%, respectively.

Based on the load-slip curves of Figs. 14 and 15, the key parameters of these curves include the maximum pull-out load P_{max}, slip value corresponding to the maximum load δ_{max}, the area under the pull-out energy diagram W_d, and the bound stress τ_{max} are given in Table 5. Also, to study the fibers performance, the stress created in them, and the strength use efficiency, which are defined as follows, are presented in Table 5.

$$\tau \frac{P_{max}}{\pi d L_{e\,max}} \tag{3}$$

$$\sigma_f = \frac{4P_{max}}{\pi d^2} \tag{4}$$

$$u_{sf} = \frac{\sigma_f}{f_{ft}} \tag{5}$$

where P_{max}, d, L_e and f_{ft} are maximum pull-out load, fiber diameter, fiber embedded length and fiber tensile strength, respectively.

The results indicate that the pull-out load and its corresponded work (area under the load-slip diagram) excess with increasing d_f and t_f for every value of r_f. It is also seen that for fibers with the radius of 0.25mm, with increasing r_f from 0 to 0.3mm, pull-out load and pull-out energy increase by 80% and 127%, respectively. According to these findings, it is observed that the maximum pull-out energy and displacement corresponding to pull-out load are seen at $r_f = 0.2$mm, and the higher r_f values show an adverse effect. Moreover, it is seen that the work needed to pull-out the RE fibers is significantly higher than the corresponding straight fibers, and is at least higher by 110%. Therefore, it can be concluded that the use of the new presented RE fibers significantly improves the pull-out performance.

The straight fibers experience bonding stress of 4.70MPa, while the RE fibers have more bond stress compared to them, which is observed to be up to 9.59MPa. In addition, by examining the u_{sf} values, it is seen that the strength use efficiency of the straight fibers is 59%, while for the RE fibers it is even more than 100% in some cases. $u_{sf} \geq 1$ shows that the maximum tensile capacity of the fibers is used, and over the pull-out mechanisim, the stress applied to the fibers is higher than their tensile strength. In these cases, the fibers will be ruptured, and as a result, the best performance is seen to be for the RE fibers.

5. Conclusions

The current research investigated the advantages of using the new steel fibers with rounded ends in reinforcing cement-based composites using a pull-out response. For this purpose, using the experimental method and the FEM, the effect of the RE fibers ends geometry on the pull-out performance of the steel fibers was studied. The interplay in the fibers and cementitious composite was investigated by employing the of the CZM concept. The parameters are gained utilizing the inverse FEM and the experimental test results performed on fiber specimens. After validating the results of the FEM with the experimental test results, the effect of the RE fibers geometric characteristics on the bonding features of the fibers with the cement composite was studied. According to the results, the following summary can be presented:

• The new presented RE fibers significantly improve the bonding behavior in comparison to conventional straight steel fibers. In this type of fibers, regarding the strong mechanical anchorage, the fibers are ruptured at their ends.

• For the same conditions, the pull-out load and absorbed energy of the RE fibers are 78% and 345%, respectively, higher compared to the straight steel fibers.

• For d_f and t_f values, respectively, greater than 0.8 and 0.5, pull-out load converges to certain values.

• Although the presence of rounded ends significantly strengthens the mechanical bonding between the fibers and cementitious composite, in the case $r_f = 0$, due to the concentration of stress, the fibers will rupture due to small amounts of pull-out load. Therefore, this type of fibers will show excellent performance in the presence of fillets at the joints. As an example, for $r_f = 0$ and $r_f = 0.2$, by increasing d_f from 0.5mm to 1mm, the pull-out load increases by 16% and 70%, respectively.

• The results show that pull-out load and total pull-out work (area under the load-slip curve) increase with increasing d_f and t_f for every value of r_f. It is also observed that for fibers with diameter of 0.5mm, with increasing r_f from 0 to 0.3mm, the pull-out load and pull-out energy increase by 80% and 127%, respectively.

Acknowledgments

The authors are grateful to Scientific Research Deanship at King Khalid University, Abha, Saudi Arabia for their financial support through the Large Research Group Project under grant number (RGP.02-230-43).

References

Abdallah, S., Fan, M. and Rees, D.W. (2018), "Bonding mechanisms and strength of steel fiber–reinforced cementitious composites: Overview", *J. Mater. Civil Eng.*, **30**(3), 04018001. https://doi.org/10.1061/(ASCE)MT.1943-5533.0002154.

Aghajanian, A., Thomas, C. and Behfarnia, K. (2021), "Effect of micro-silica addition into electric arc furnace steel slag eco-efficient concrete", *Appl. Sci.*, **11**(11), 4893. https://doi.org/10.3390/app11114893.

Aghakhani, M. and Naderian, P. (2015), "Modeling and optimization of dilution in SAW in the presence of Cr2O3 nano-particles", *Int. J. Adv. Manuf. Technol.*, **78**(9), 1665-1676. https://doi.org/10.1007/s00170-014-6733-3.

Baniya, H.B., Guragain, R.P., and Subedi, D.P. (2021), "Cold atmospheric pressure plasma technology for modifying polymers to enhance adhesion: A critical review", *Rev. Adhes. Adhes.*, **9**(2), 269-307. https://doi.org/10.7569/RAA.2021.097306.

Dahi Taleghani, A., Ahmadi, M. and Olson, J.E. (2013), "Secondary fractures and their potential impacts on hydraulic fractures efficiency", *Proceedings of the ISRM International Conference for Effective and Sustainable Hydraulic Fracturing*, OnePetro. https://doi.org/10.5772/56360.

Dhiman, N.K., Sidhu N., Agnihotri S., Mukherjee A. and Reddy M.S. (2022), "Role of nanomaterials in protecting building materials from degradation and deterioration", *Biodegr. Biodeterior. Nanosc.*, **5**, 405-475. https://doi.org/10.1016/B978-0-12-823970-4.00024-5.

Ding, X., Geng, H., Zhao, M., Chen, Z. and Li, J. (2021), "Synergistic bond properties of different deformed steel fibers embedded in mortars wet-sieved from self-compacting SFRC", *Appl. Sci.*, **11**(21), 10144. https://doi.org/10.3390/app112110144.

Dmytro, S. (2020), "The study of welding requirements during construction and installation of seismic-resistant steel structures", *J. Res. Sci. Eng. Technol.*, **8**(2), 17-20.

Du, J., Meng, W., Khayat, K.H., Bao, Y., Guo, P., Lyu, Z. and Wang, H. (2021), "New development of ultra-high-performance concrete (UHPC)", *Compos. Part B Eng.*, **224**, 109220. https://doi.org/10.1016/j.compositesb.2021.109220.

Ebrahimi, F., and Habibi, S. (2017), "Low-velocity impact response of laminated FG-CNT reinforced composite plates in thermal environment", *Adv. Nano Res.*, **5**(2), 69. https://doi.org/10.12989/anr.2017.5.2.069.

Esmaeili, J., Andalibi, K., Gencel, O., Maleki, F. K. and Maleki, V. A. (2021), "Pull-out and bond-slip performance of steel fibers with various ends shapes embedded in polymer-modified concrete", *Constr. Build. Mater.*, **271**, 121531. https://doi.org/10.1016/j.conbuildmat.2020.121531.

Esmaeili, J. and K. Andalibi (2019), "Development of 3D Meso-Scale finite element model to study the mechanical behavior of steel microfiber-reinforced polymer concrete", *Comput. Concr.*, **24**(5), 413-422. https://doi.org/10.12989/cac.2019.24.5.413.

Graybeal, B.A. (2008), "Flexural behavior of an ultrahigh-performance concrete I-girder", *J. Bridge Eng.*, **13**(6), 602-610. https://doi.org/10.1061/(ASCE)1084-0702(2008)13:6(602).

Jarach, N., Zuckerman, R., Naveh, N., Dodiuk, H., and Kenig, S. (2021), "Bio-and water-based reversible covalent bonds containing polymers (vitrimers) and their relevance to adhesives", *Rev. Adhes. Adhes.*, **9**(1). https://doi.org/10.7569/RAA.2021.097302.

Kaloop, M.R., Abd Elrahman, M. and Hu, J.W. (2022), "Nondestructive tests for defections detection of nanoparticles in cement-based materials: A review," *Adv. Nano Res.*, **12**(1), 1-23. https://doi.org/10.12989/anr.2022.12.1.001.

Kim, J.J., Yoo, D.Y. and Banthia, N. (2021), "Benefits of curvilinear straight steel fibers on the rate-dependent pullout resistance of ultra-high-performance concrete", *Cement Concr. Compos.*, **118**, 103965. https://doi.org/10.1016/j.cemconcomp.2021.103965.

Lee, S.J., Eom, A.H., Ryu, S.J. and Won, J.P. (2016), "Optimal dimension of arch-type steel fibre-reinforced cementitious composite for shotcrete", *Compos. Struct.*, **152**, 600-606. https://doi.org/10.1016/j.compstruct.2016.05.099.

Rajeshkumar, S., Subramanian, A.K. and Prabhakar, R., (2021), "In vitro Anti-inflammatory activity of Silymarin/

Hydroxyapatite/Chitosan Nanocomposites and its cytotoxic effect using Brine shrimp lethality assay: Nanocomposite for biomedical applications", *J. Popul. Therapeut. Clin. Pharmacol.*, **28**(2). https://doi.org/10.47750/jptcp.2022.874.

Maleki, F.K., Nasution, M.K., Gok, M.S. and Maleki, V.A. (2022), "An experimental investigation on mechanical properties of Fe2O3 microparticles reinforced polypropylene", *J. Mater. Res. Technol.*, **16**, 229-237. https://doi.org/10.1016/j.jmrt.2021.11.104.

Ming, M., Zheng, S., Zhang, Y., Zheng, Y., Yang, S. and Song, M. (2021), "Experimental study on the bond-slip behavior and stress transfer mechanism between shaped steel and high-performance fiber-reinforced concrete", *Structures*, **34**, 5013-5028. https://doi.org/10.1016/j.istruc.2021.09.014.

Müssig, J. and Graupner, N. (2021), "Test methods for fibre/ matrix adhesion in cellulose fibre-reinforced thermoplastic composite materials: A critical review", *Rev. Adhes. Adhes.*, **8**(2), 68-129. https://doi.org/10.7569/RAA.2020.097306.

Naderi, S. and Zhang, M. (2022), "3D meso-scale modelling of tensile and compressive fracture behaviour of steel fibre reinforced concrete", *Compos. Struct.*, **291**, 115690. https://doi.org/10.1016/j.compstruct.2022.115690.

Parashar, A.K. and Gupta, A. (2021), "Investigation of the effect of bagasse ash, hooked steel fibers and glass fibers on the mechanical properties of concrete", *Mater. Today Proceedings*, **44**, 801-807. https://doi.org/10.1016/j.matpr.2020.10.711.

Poveda, E., Yu, R.C., Tarifa, M., Ruiz, G., Cunha, V.M. and Barros, J.A. (2020), "Rate effect in inclined fibre pull-out for smooth and hooked-end fibres: A numerical study", *Int. J. Fract.*, **223**(1), 135-149. https://doi.org/10.1007/s10704-019-00404-7.

Qi, J., Wu, Z., Ma, Z.J. and Wang, J. (2018), "Pullout behavior of straight and hooked-end steel fibers in UHPC matrix with various embedded angles", *Constr. Build. Mater.*, **191**, 764-774. https://doi.org/10.1016/j.conbuildmat.2018.10.067.

Rezaee, M. and Maleki, V.A. (2015), "An analytical solution for vibration analysis of carbon nanotube conveying viscose fluid embedded in visco-elastic medium", *Proceedings of the Institution of Mechanical Engineers, Part C: Journal of Mechanical Engineering Science*, **229**(4), 644-650. https://doi.org/10.1177/0954406214538011.

Riahi, S., Nemati, A., Khodabandeh, A.R. and Baghshahi, S. (2021), "Investigation of interfacial and mechanical properties of alumina-coated steel fiber reinforced geopolymer composites", *Constr. Build. Mater.*, **288**, 123118. https://doi.org/10.1016/j.conbuildmat.2021.123118.

Sharma, R., Jang, J.G. and Bansal, P.P. (2022), "A comprehensive review on effects of mineral admixtures and fibers on engineering properties of ultra-high-performance concrete", *J. Build. Eng.*, **45**, 103314. https://doi.org/10.1016/j.jobe.2021.103314.

Shekhovtsova, S. and Korolev E. (2022), "Interfacial phenomena at the interface in the system «carbon primary materials-water solutions of surfactants» for cement materials", *Materials*, **15**(2), 556-587. https://doi.org/10.3390/ma15020556.

Sher, F., Hazafa A., Rashid T., Bilal M., Zafar F., Mushtaq Z. and Nisa Z.U. (2022), "Effects of zeolite-based nanoparticles on the biodegradation of organic materials", *Biodegr. Biodeter. Nanosc.*, **134**, 579-601. https://doi.org/10.1016/B978-0-12-823970-4.00021-X.

Schmidt, M., and Fehling, E. (2005), "Ultra-high-performance concrete: Research, development and application in Europe", *ACI Spec. Publ*, **228**(4), 51-78. https://doi.org/10.14359/14460.

Tai, Y.S., Kim, J.J., Yoo, D.Y. (2020), "Spacing and bundling effects on rate-dependent pullout behavior of various steel fibers embedded in ultra-high-performance concrete", *Arch. Civil Mech. Eng.*, **20**(2), 1-18. https://doi.org/10.1007/s43452-020-00048-8.

Timesli, A. (2021), "A cylindrical shell model for nonlocal buckling behavior of CNTs embedded in an elastic foundation under the simultaneous effects of magnetic field, temperature change, and number of walls", *Adv. Nano Res.*, **11**(6), 581-593. https://doi.org/10.12989/anr.2021.11.6.581.

Wille, K., Naaman, A.E., El-Tawil, S. and Parra-Montesinos, G.J. (2012), "Ultra-high performance concrete and fiber reinforced concrete: Achieving strength and ductility without heat curing", *Mater. Struct.*, **45**(3), 309-324. https://doi.org/10.1617/s11527-011-9767-0.

Won, J.P., Lee, J.H. and Lee, S.J. (2015), "Flexural behaviour of arch-type steel fibre reinforced cementitious composites", *Compos. Struct.*, **134**, 565-571. https://doi.org/10.1016/j.compstruct.2015.08.092.

Yang, L., Caijun S. and Zemei, W. (2019), "Mitigation techniques for autogenous shrinkage of ultra-high-performance concrete–A review", *Compos. Part B Eng.*, **178**, 107456. https://doi.org/10.1016/j.compositesb.2019.107456.

Zerrouki, R., Karas, A., and Zidour, M. (2020), "Critical buckling analyses of nonlinear FG-CNT reinforced nano-composite beam", *Adv. Nano Res.*, **9**(3), 211-220. https://doi.org/10.12989/anr.2020.9.3.211.

SR